energies

MDPI

Article

Identification of Reservoir Water-Flooding Degrees via Core Sizes Based on a Drip Experiment of the Zhenwu Area in Gaoyou Sag, China

Xiaoyu Ju [1,2,*], Xiaodong Zhao [3,*], Boyu Zhou [4], Ruixue Zhang [5], Xinyu Wu [4] and Dafa Guo [3]

1 School of Economics and Management, China University of Petroleum (Beijing), Beijing 102249, China
2 School of Business Administration, China University of Petroleum (Beijing) at Karamay, Karamay 834000, China
3 School of Petroleum, China University of Petroleum (Beijing) at Karamay, Karamay 834000, China
4 Exploration and Development Research Institute, Xinjiang Oilfield Company, CNPC, Karamay 834000, China
5 Exploration and Development Research Institute, Huabei Oilfield Company, CNPC, Renqiu 062550, China
* Correspondence: juxiaoyu@cupk.edu.cn (X.J.); zhaoxd2019@cupk.edu.cn (X.Z.)

Abstract: In order to identify the degree of water flooding in a reservoir and to discover any remaining oil-enriched areas, in this paper, a systematic study on the water flooding of cores in obturated coring wells is carried out. With observations and testing data of the cores, based on the notion of sedimentary facies, the water-flooding degrees of 4–7 sand groups in member one of the Paleogene Sanduo Formation ($E_2s_1^{4-7}$) of the Zhenwu area in the Gaoyou Sag are determined. Overall, the results show that the study area is formed under the background of lake regression, with various sedimentary systems, mainly including delta facies, braided fluvial facies, and meandering fluvial facies. The degree of water flooding is determined using a point-by-point drip experiment of the core. Combined with the testing results of the core, the water-flooding degrees of the different sedimentary facies are quantitatively determined. Identification standards for the water-flooding degree of delta facies, braided river facies, and meandering river facies are established. The water-flooding degree of the delta sand body is generally weak, with an oil saturation rate of 24.1–40.2%, essentially indicating no water flooding or weak water flooding. The water-flooding degree of the braided fluvial sand body significantly changes, and the variation range of the oil and water saturation measurement results is also large. The water-flooding degree of the meandering fluvial sand body is weaker than that of the braided fluvial sand body, which is mostly not flooded or weakly flooded. The water-flooding degree is obviously controlled by the sedimentary rhythm and the sedimentary type. The top of the positive rhythm, the bottom of the sludge bed in the braided fluvial point bar, the deltaic front subaqueous distributary channel, and the point bar in the meandering fluvial have relatively low water-flooding degrees. They are the subjects of subsequent development adjustment and the remaining oil potential tapping.

Keywords: drip experiment; core size; water-flooding degree; sedimentary rhythm; sedimentary type

check for updates

Citation: Ju, X.; Zhao, X.; Zhou, B.; Zhang, R.; Wu, X.; Guo, D. Identification of Reservoir Water-Flooding Degrees via Core Sizes Based on a Drip Experiment of the Zhenwu Area in Gaoyou Sag, China. *Energies* **2023**, *16*, 608. https://doi.org/10.3390/en16020608

Academic Editor: Reza Rezaee

Received: 26 November 2022
Revised: 22 December 2022
Accepted: 26 December 2022
Published: 4 January 2023

Copyright: © 2023 by the authors. Licensee MDPI, Basel, Switzerland. This article is an open access article distributed under the terms and conditions of the Creative Commons Attribution (CC BY) license (https://creativecommons.org/licenses/by/4.0/).

1. Introduction

The identification of a reservoir's degree of water flooding is one of the most important research topics of the late development adjustment and remaining oil tapping of high water-cut oilfields [1–3]. In recent years, many scholars have studied and evaluated flooded layers from various perspectives, and the introduction of mathematical methods has promoted the quantitative evaluation of flooded layers [4–7]. Zhang et al. believed that, with the help of dynamic development information in relation to sand bodies connected between water injection wells and production wells in the process of reservoir water injection development, the water-flooding degrees of sand bodies can be analyzed to a certain extent [8]. He et al. verified the relationship between the hydrocarbon ratio

(RCH) and porosity and oil saturation, and they proposed that the remaining oil and water-flooding degrees can be evaluated using hydrocarbon ratio logging technology [9]. Shen et al. proposed identification methods and standards for different water-flooding levels of ultra-low-permeability reservoirs, according to the response characteristics of conventional logging and nuclear magnetic logging [10]. Ren et al. used production profile data to determine the remaining oil saturation levels in a water-flooded layer, and they built a saturation model map of the non-uniform water-flooded layer using the area equivalent method [11]. Shi et al. proposed a method to identify water-flooded layers using reconstructed resistivity curves [12]. Miao et al. proposed a method to quantitatively identify water-flooded zones by combining crude oil saturation, movable oil saturation, and residual oil saturation [13]. Lang et al. established a method to analyze the oil saturation levels of a core and the water-flooded layer using diffusion relaxation two-dimensional spectrum technology [14]. These methods are basically used to judge the degree of water flooding based on logging curves and log interpretation, which belong to the study of secondary data; thus, the knowledge surrounding water-flooded layers is limited.

The cores obtained via closed coring are essentially free from the pollution of drilling fluids. A sealed core can truly reproduce the original geological porosity, oil saturation, water invasion, and water cut of the formation [15,16]. However, in this paper, the most intuitive identification method was used to observe whether the core of a sealed coring well is flooded, that is, a drip test. This idea was realized in the Zhenwu area of the Gaoyou Sag. Based on the analyses and test data of cores, core observations were made, and water dripping experiments were implemented on the basis of sedimentary understanding. The water-flooding degrees of different sedimentary sand bodies in sealed coring wells were also analyzed. A relational chart was then established based on the analysis and test results of the cores, and the water-flooding degrees of the different sedimentary sand bodies were quantitatively identified. Finally, the influence of deposition on water-flooding degrees was clarified to lay the foundation for increasing reserves and production in high water-cut oilfields and for adjusting development plans. This paper mainly analyzed the influence of the sedimentary rhythm and sedimentary type on water-flooding degrees.

2. Geological Setting

Zhenwu Oilfield is located in the south of the Gaoyou Sag in the Subei Basin, eastern China (Figure 1a). The structure is a rolling anticline structure formed by the reverse traction of the large fault Zhen 2 (Figure 1b) [17]. The reservoir is mainly controlled by both structure and lithology, and it is a structural sandstone reservoir with medium–high porosity and medium–high permeability. The study area derives a series of secondary faults from the large fault Zhen 2, which is a complex fault block area (Figure 1c). The research area is one of the main oil-bearing strata, and it has entered a stage of decline. The sedimentary environment is in the transition period from a lake environment to a river environment [18]. It has a complex deposition, mainly in relation to the transitional sedimentary system of fluvial delta facies [19]. The burial depth of the reservoir is 1750~2000 m, and it has a set of sand–shale interbed strata. The $E_2s_1^{4-7}$ sand group is divided into 24 sub-layers, including 16 main sub-layers, mainly concentrated in the 6~7 sand group. The oilfield began to inject water in 1978. Currently, the cumulative water injection rate exceeds 3250.52×10^4 t. At present, the number of drilling wells in the study area is more than 250, the number of injection wells is 77, and the comprehensive water content is more than 90% [20].

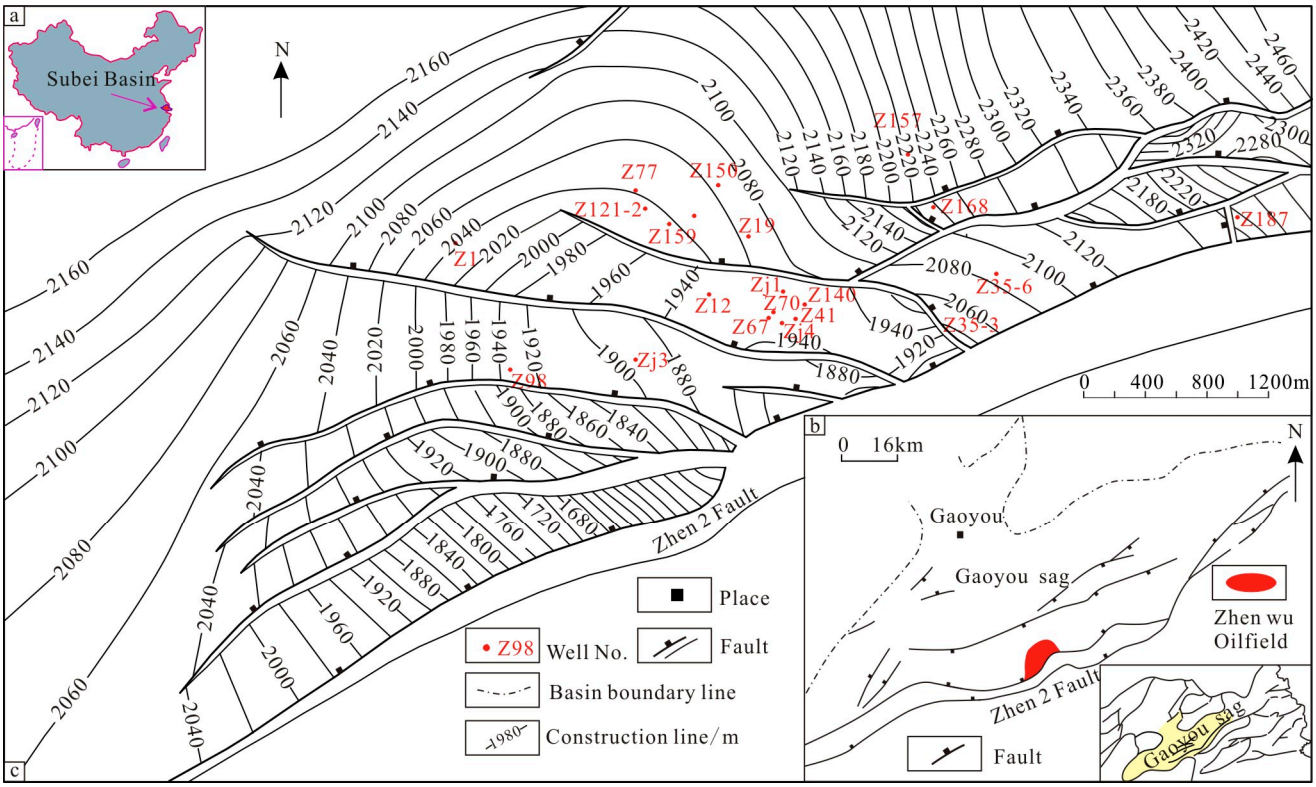


Figure 1. Tectonic underside structure and coring well distribution position of $E_2s_1^{4-7}$ in the Zhenwu area, Gaoyou Sag. (**a**) Location of the Subei Basin in the east of China; (**b**) location of Gaoyou Sag; (**c**) sketch of Zhenwu Oilfield.

3. Materials and Methods

Core data can truly and objectively reflect the latest underground situation. Detailed observations and analyses of 21 coring wells in the $E_2s_1^{4-7}$ sand group in the Zhenwu area, Gaoyou Sag, were conducted. In this research, through a drip experiment, observations were made for the first time regarding whether the sealed rock core is flooded point by point. The specific working process is as follows: at the oilfield coring site, a drop of water was taken with a drip bottle and dropped on the flat and fresh surface of an oil-bearing core, and then the shape and infiltration of the water drops were observed [21,22]. The drip experiment must be carried out on the fresh surface of a split core. On-site drip tests of oil-bearing and water-bearing cores can be divided into four levels: fast-drip penetration, slow-drip penetration, micro-drip penetration, and no-drip penetration [23]. The rapid infiltration of dripping water is immediate infiltration after dripping, and it provides characteristics of a water layer. The slow seepage of dripping water means that the water drops diffuse immediately or slowly after dripping. The surfaces of the water drops are flat, with the characteristics of oil-bearing water layers. Micro-drip permeability means that the surfaces of the water drops are steamed in a bread-like way, and the saturation angle is 60~90°, which is basically impermeable, suggesting that there is no or a limited amount of water and, in turn, providing the characteristics of water-bearing oil layers or dense layers. Water-dripping impermeability refers to the surfaces of water drops that are in a bad shape or an oblate shape, whereby the saturation angle is greater than 90°, and the water drops roll in the rock, indicating that there is no free water at all and, in turn, providing the characteristics of an oil-only layer. No-drip penetration means no water flooding, micro-drip penetration means weak water flooding, slow-drip penetration means medium water flooding, and fast-drip penetration means strong water flooding [24,25]. According to this workflow and judgment criteria, the degree of flooding can be effectively judged.

Zhenjian 4 is a well located in the Zhenwu Oilfield. The sealed coring of the study layer was carried out in this well. The total number of coring times is 13, the total footage is 82.17 m, the core length is 81.03 m, the harvest rate is 98.61%, and the sealing rate is 89.13%. We carried out a detailed core observation and a water-dripping experimental analysis of the well. In total, 157 samples were taken in the study section, and the oil and water saturation, porosity, and permeability rates of the samples were then measured. The reservoir physical properties, namely, porosity and permeability, were determined using a gas porosity tester and a gas permeability tester, respectively, in the testing environment, with a temperature of 20 °C and a humidity of 52%. The test methods, processes, and test results meet the national standard SY/T 5336-2006 of China (https://www.cssn.net.cn/, accessed on 25 November 2022). In addition, oil saturation was determined using atmospheric distillation. Specifically, in the process of high-temperature retorting, the oil–water existing in the crushed fresh rock sample first turns into steam and then condenses before being collected into a liquid production pipe in order to determine the saturation. Because the core used in this study has sealed coring and is not polluted by drilling fluid, the core filtrate invasion had no influence on the saturation. According to the saturation measurement results, the water-flooding degree of the core scale can be quantitatively identified based on different sedimentary facies types.

4. Results

4.1. Understanding of Sedimentary Facies

A detailed observation and an analysis of 21 coring wells in the study area show that fluvial delta facies deposits developed in the $E_2s_1^{4-7}$ sand group in the Zhenwu area, Gaoyou Sag. The $E_2s_1^{7}$ sand group located in the lower part developed delta facies, and the $E_2s_1^{6}$ sand group developed braided fluvial facies. Meandering fluvial facies developed in the upper $E_2s_1^{4}$ and $E_2s_1^{5}$ sand groups, comprising a set of multi-type deposits formed under the background of lake regression. The sedimentary microfacies in the study area had the characteristics of a fast sedimentary phase transition and multiple sedimentary types.

4.1.1. The Symbol of Depositional

The Color of Mudstone

The mudstone color of the $E_2s_1^{4-7}$ sand group was mainly found to be dark, miscellaneous, and brown. Among them, brown reflects the sedimentary characteristics of an aquatic oxidation environment, dark reflects the sedimentary characteristics of an underwater reduction environment, and miscellaneous reflects the sedimentary characteristics of the semi-oxidation and semi-reduction of effluent (Figure 2a). From the bottom to the top, the mudstone color gradually becomes lighter, reflecting that the E_2s_1 sedimentary system generally has the characteristics of lake facies in transition-to-continental facies.

Rock Type, Structure, and Composition

The rock types are mainly medium-fine sandstone and fine sandstone. Common gravel-bearing sandstone and glutenite characteristics are also reported. Overall, there are also coarse grains, small lithology changes, and high structural maturity levels (Figure 2b,c). Under microscopic conditions, the sandstone is dominated by lithic feldspathic sandstone. Quartz, feldspar, and lithic are the main clastic components, whereby the latter accounts for 21.3% of particle support, reflecting the low maturity of the reservoir components.

Sedimentary Tectonics

The core observation shows that the sedimentary structure types are mainly staggered bedding, parallel bedding, scour-and-fill structures, and biological disturbance (Figure 2d). The progradation direction of the interlaced bedding midrib shows the direction of the channel flow. Parallel bedding is generally formed under the hydrodynamic conditions of shallow water and rapid flow, and a scour-and-fill structure is also a kind of stratification structure formed under high-flow states, both of which reflect the hydrodynamic mecha-

nism of the strong traction flow. Moreover, biological disturbance often occurs in shallow water sedimentary environments, which are rich in organisms.

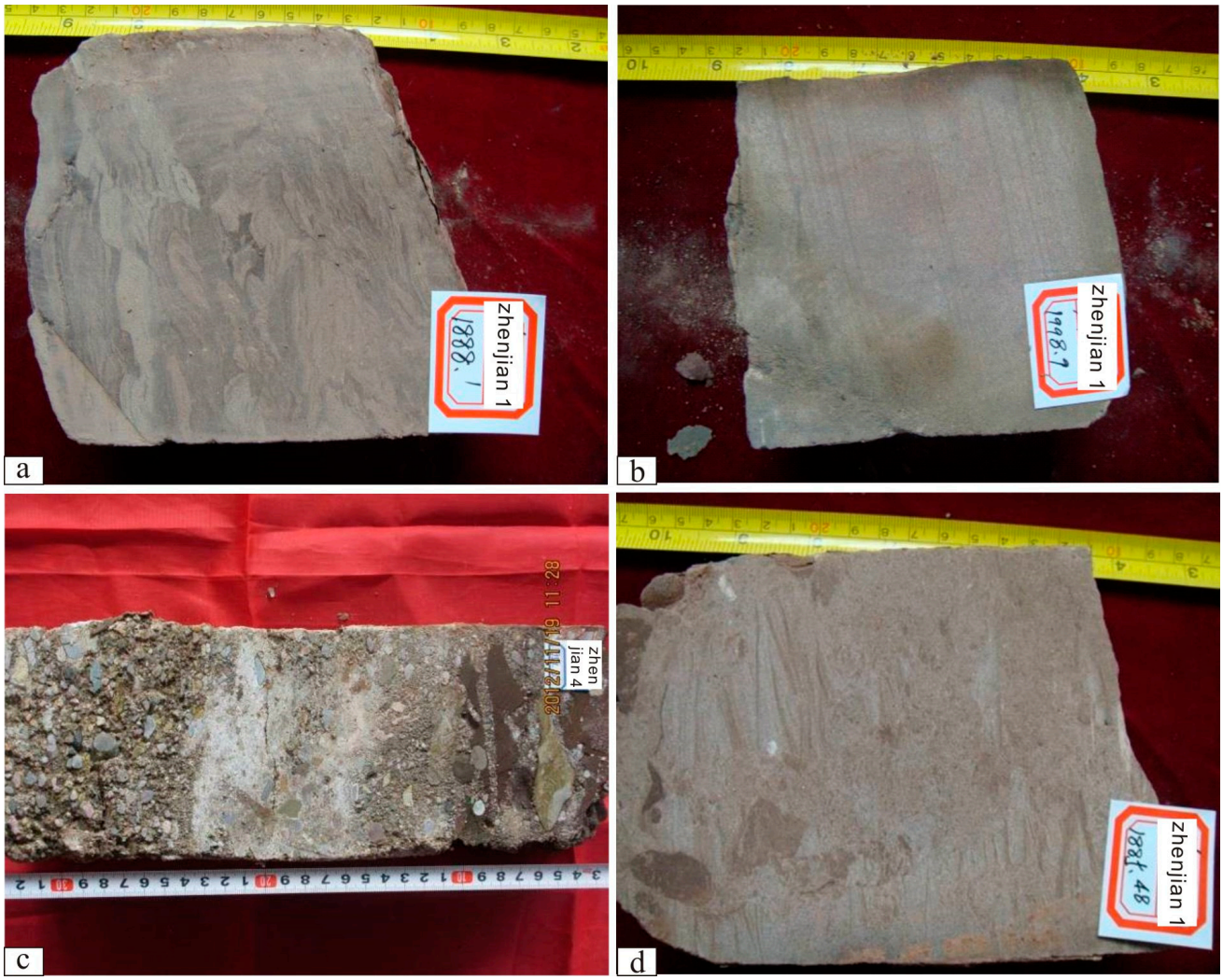


Figure 2. Typical sedimentary structure of $E_2s_1^{4-7}$ in the Zhenwu area, Gaoyou Sag. (**a**) Zhenjian 1 well, cross-bedding, 1888 m; (**b**) Zhenjian 1 well, parallel bedding, 1998.9 m; (**c**) Zhenjian 4 well, scour-and-fill structure, 1951.65 m; (**d**) Zhenjian 1 well, bioturbation, 1885.48 m.

Logging Response Characteristics

The natural potential curves of the study area are bell-shaped, box-shaped, tooth-shaped, and finger-shaped with composite forms (Figure 3). The bell-shaped curve shows that the bottom erosion surface is abruptly contacted and that the top is gradually contacted, which mainly reflects the deposition of the underwater distributary channel sand body. The box curve shows the rich provenance and stable hydrodynamic conditions in the deposition process, which mainly reflect the sedimentary environment of the river. The toothed box curve indicates that there is a deposition layer in the interior, which generally relates to heart beach deposition. The finger-shaped curve shows that the sedimentary environment energy is weak and that the provenance is minimal, which is usually indicative of natural levee or sheet sand deposition.

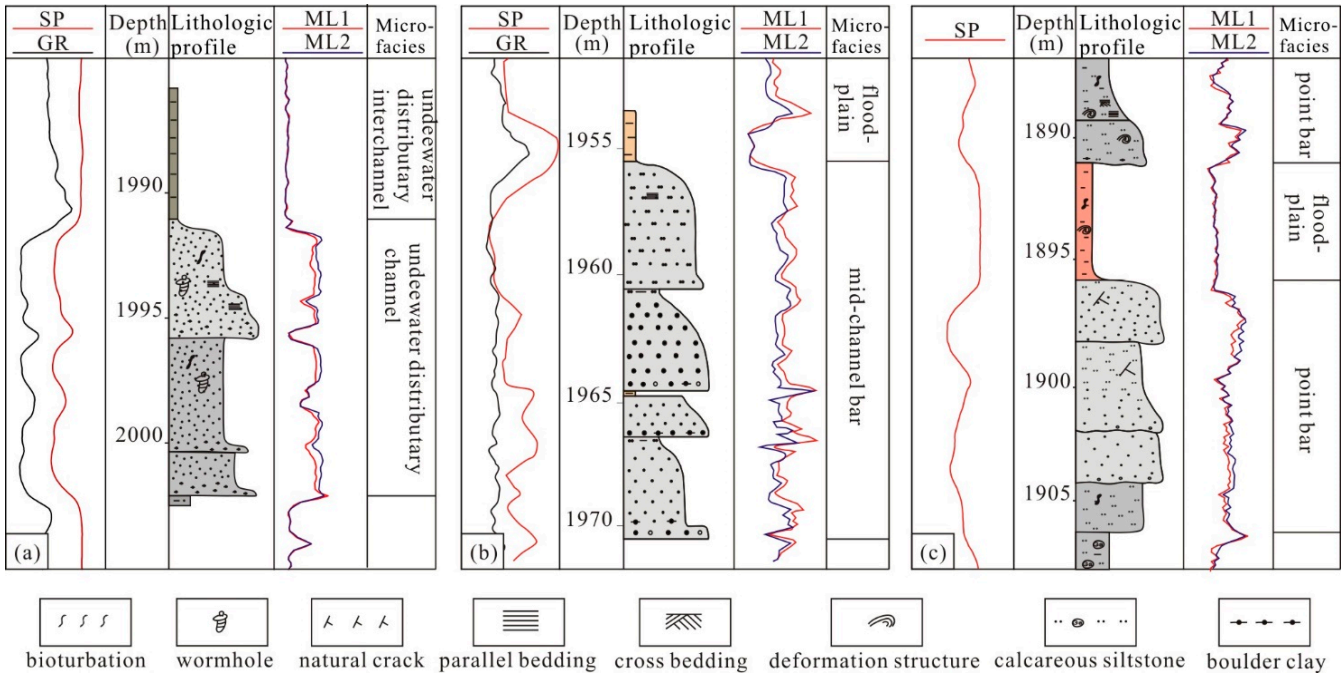


Figure 3. The main sedimentary microfacies characteristics of $E_2s_1^{4-7}$ in the Zhenwu area, Gaoyou Sag. (**a**) Zhenjian 4, delta facies; (**b**) Zhen 140, braided fluvial facies; (**c**) Zhenjian 1, meandering fluvial facies.

4.1.2. Types and Characteristics of Sedimentary Facies

Based on the regional geological background and previous studies, in light of the core observations, various sedimentary facies marks, single-well sedimentary facies, well-connected section facies, and the plane distribution characteristics of the sedimentary facies, three sedimentary delta, braided fluvial, and meandering fluvial facies were identified in E2s1 in the Zhenwu area in Gaoyou Sag, and ten heart beach, edge beach, mouth bar, and channel microfacies were also identified (Figure 3).

Delta Facies

The delta facies mainly developed in the $E_2s_1^7$ sand group in the study area, and the delta-front subfacies are relatively well-developed, pertaining to the belts of the main sedimentary sand bodies of the delta facies. The most common types of sedimentary microfacies are underwater distributary channels, mouth bars, sheet sand, underwater distributary bays, etc. The main characteristics of the sedimentary microfacies and subaqueous distributary channel microfacies relate to the belt of the underwater extension facies within the distributary channel of the delta plain subfacies. The grain size of the sediments is fine, and the sorting is medium-to-good. The sediments are mainly composed of sand, fine sand, and silt, with a small amount of argillaceous sediment, and they often develop wavy interlaced bedding and scour-and-fill structures. Subaqueous interdistributary bay microfacies mainly consist of gray mudstone, impure textures, silt bands, and wavy bedding. Due to river erosion, the thickness of the mudstone between rivers changes significantly, and some regions are even completely eroded, thus indicating that the channel sand bodies are directly contacted at different periods of time.

Braided Fluvial Facies

Braided fluvial sedimentary facies mainly consist of gravel, and they are subject to the coarse sand deposition of the positive cycle deposition, developed in the $E_2s_1^6$ sand group. Braided fluvial sedimentary facies can also be divided into riverbed subfacies and flood subfacies. Riverbed subfacies can then be divided into braided channel and

core beach sedimentary microfacies, while flood subfacies are mainly flood plains. The main characteristics of sedimentary microfacies and heart beach microfacies are as follows: a gray to gray-white color and a grain size similar to that of coarse-grained and fine-grained siltstone and lithic sandstone, respectively. The composition maturity is low, the sorting of the sandstone is poor, and the thickness reaches 10~20 m, showing an inverse grain order. The sedimentary structure is dominated by large-scale interlaced bedding and wavy bedding, and the gravel is visible locally. In braided channel microfacies, the lithology is coarse, mainly comprising coarse sandstone and glutenite, as well as gravel sandstone with a small amount of medium-coarse conglomerate. Furthermore, the size of the gravel is mixed, and the composition is complex. The diameter of the gravel is 0.5~3 cm. The sorting is medium-to-poor. The grinding circle is sub-angular to sub-circular. The interstitial materials are mainly argillaceous, micro-gravel, and coarse sand. In the bottom erosion surface, the gravel is imbricate with a normal sequence deposition, and a common sedimentary structure mainly develops with block bedding, parallel bedding, and staggered bedding.

Meandering Fluvial Facies

Meandering fluvial sedimentary facies mainly develop in the $E_2s_1^{4-5}$ sand layer group. According to a comprehensive analysis of various factors, such as core observation and sand body plane distribution, the meandering fluvial sedimentary facies are divided into two subfacies, namely, riverbed subfacies and flood subfacies, which can then be subdivided into five microfacies: beaches, meandering river channels, natural levees, crevasse fans, and flood plains. The main characteristics of beach microfacies are also described. Beach, one of the many types of microfacies, has the largest thickness of any sand body in meandering fluvial facies, and its rock type is mainly medium-fine lithic feldspar sandstone. The quartz content in the rock is about 50~60%, while its feldspar content is about 30~35%. It is also a low-maturity type of sandstone. The median grain size of the sandstone is generally 0.15~0.2 mm. Slot-like interlaced bedding is found in the beach sediments, and bottom erosion generally occurs at the bottom of the sand body. In the microfacies of meandering fluvial facies, sandstone is the main rock type, followed by glutenite. The detrital particles of meandering fluvial facies are coarse, their bedding is well-developed, there are many types, they do not develop animal and plant fossils, and they only supply broken plant branch debris. The sand body is zonally distributed with good connectivity, and its bottom scour surface is discernable.

4.2. Analysis of Core Dripping

The core of the Zhenjian 4 well, extracted three times at 1985.82~2002.43 m in the well section, has a length of 16.61 m. This section is centered around the delta-front deposition, and it has an underwater distributary channel and underwater interdistributary bay microfacies. Water dripping was carried out on the oil sand core of this section at 1993.09 mm, 1998.14 m, and 2000.10 m, demonstrating that the core is cylindrical and that there is no-drip penetration (Figure 4a–c), thus indicating that the water-flooding degree of this section is generally weak. Five cores were extracted at 1929.40~1968.47 m in the well section, and the core length is 38.56 m. The core of this section is braided fluvial deposition, and it is dominated by core beach and braided channel microfacies. Fast-drip penetration was observed in the cores of 1939.01 m and 1941.37 m in the upper part of this section (Figure 4d).

In the middle of 1947.39 m and 1949 m, the core drops are cylindrical (Figure 4e); however, the core at the lower part of 1955.31 m was noted to be impermeable by dripping water (Figure 4f), but the core at the bottom of 1966.66 m is cylindrical due to dripping water (Figure 4g). The core has a fine particle size and low porosity, and there is a 2 m non-permeable sediment layer at the top of the core. The water-flooding degree in the middle of the segment is weak, and the water-flooding degree in the top and bottom is strong. Affected by the non-permeable sediment layer at the bottom, there is also a water-flooded

layer of about 2 m. The water-flooding degree is mainly related to the sedimentary rhythm and the sediment layer. In the well section (1881.00~1907.49 m), five cores were extracted, and the core length is 25.86 m. The core in this section is of a meandering fluvial deposition, and the existence of microfacies of beaches, meandering fluvial facies, and flood plains was noted. At 1886.26 m, the impermeable core dripping is cylindrical (Figure 4h), and at 1903.78 m, the core dripping is slight and hemispherical (Figure 4i). This indicates that the water-flooding degree of the core in this section is generally weak, but there are differences among the various cores. Overall, the flooding degree of the delta facies and meandering fluvial facies is weak, while that of the braided fluvial facies is strong. However, the degree of flooding of the sand bodies in the same sedimentary type is uneven.

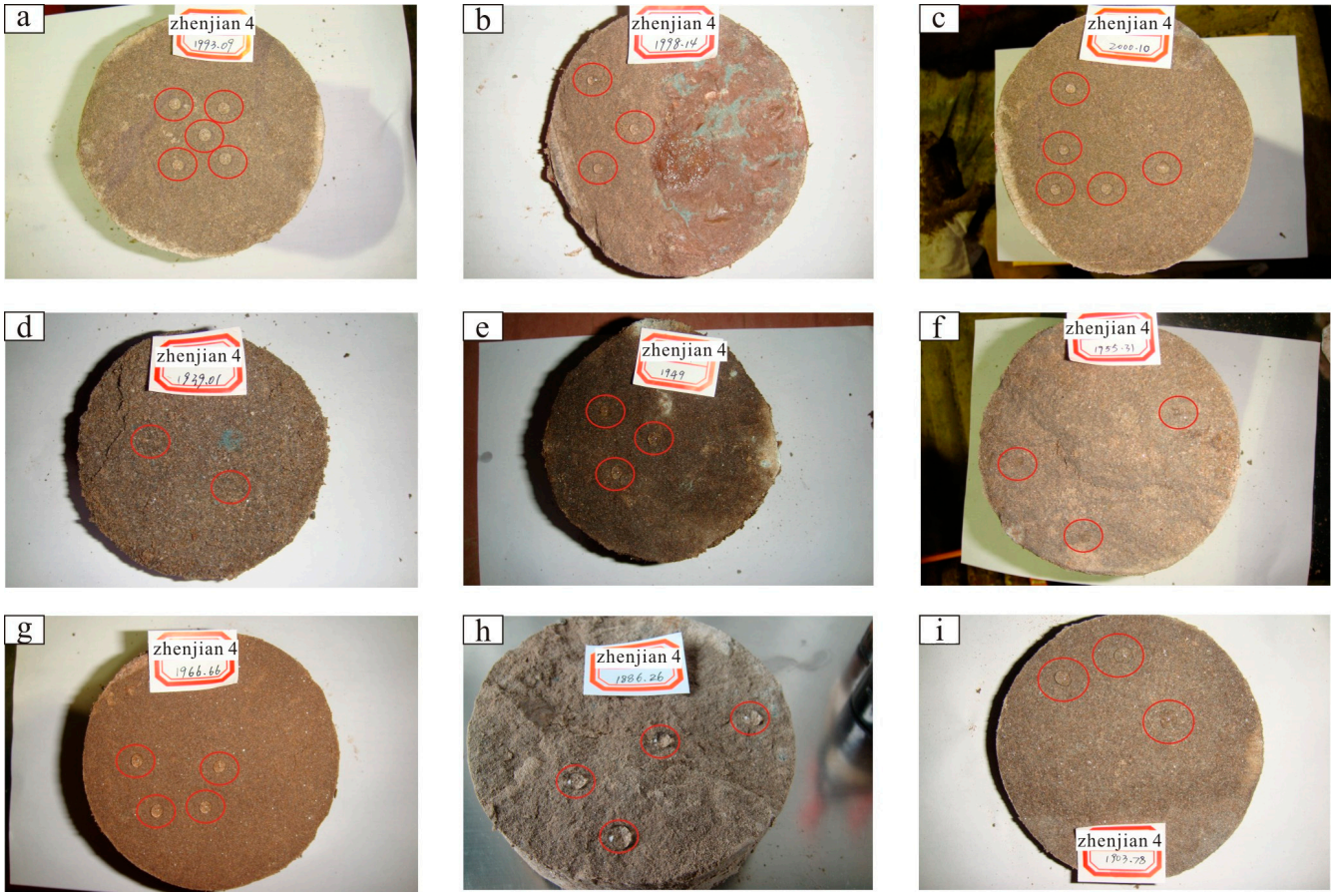


Figure 4. Drip characteristics of core section sand body in Zhenjian 4. (**a**) The Zhenjian 4 well (1993.09 m) shows that the core is cylindrical after water dripping, and no-drip penetration was observed; (**b**) the Zhenjian 4 well (1998.14 m) shows that the core is cylindrical after water dripping, and no-drip penetration was observed; (**c**) the Zhenjian 4 well (2000.1 m) shows that the core is cylindrical after water dripping, and no-drip penetration was observed; (**d**) in the Zhenjian 4 well (1939.01 m), fast-drip penetration was observed; (**e**) in the Zhenjian 4 well (1949 m), no-dripping was observed; (**f**) in the Zhenjian 4 well (1955.31 m), fast-drip penetration was observed; (**g**) in the Zhenjian 4 well (1966.66 m), no-drip penetration was observed; (**h**) in the Zhenjian 4 well (1886.26 m), no-drip penetration was observed; (**i**) in the Zhenjian 4 well (1903.78 m), water dripping was noted to be slight and hemispherical.

5. Discussion

5.1. Flooding Degree Identification

The water-flooding degree of different oil sand bodies was identified via an analysis of water dripping in the core of Zhenjian 4. According to the degree of water drop penetration, the water-flooding degree was divided into four types: no water flooding,

weak water flooding, medium water flooding, and strong water flooding. The criteria for judging the degree of water flooding are as follows: no infiltration of water-flooding drops, weak infiltration of water-flooding drops, medium infiltration of water-flooding drops, and strong infiltration of water-flooding drops. Using qualitative judgment standards, the water-flooding degree of each oil sand body was identified, and then the relationship between the water-flooding degree and the measured results of the oil and water saturation was established. The water-flooding degree of the different sedimentary facies was quantitatively identified, and a water-flooding degree recognition standard suitable for the study area was established. Evidently, there is a certain relationship between the water-flooding degree of the core and the oil and water saturation. Generally, the higher the oil saturation and the lower the water saturation, the weaker the water-flooding degree of the sand body. Furthermore, the lower the oil saturation and the higher the water saturation, the stronger the water-flooding degree of the sand body [26,27]. This is because the saturation of the sand body changes dynamically during the development of high water-cut oilfields via water injection, and different reservoirs are washed to different degrees. For the same sedimentary reservoir, the degree of washing can be strong and weak, and the remaining oil can be not enriched and enriched, respectively, which is manifested in the changes in the oil content and water saturation [28–30].

Based on the core dripping analysis combined with the results of the oil and water saturation measured via experiments, identification standards for the water-flooding degree of delta facies, braided fluvial facies, and meandering fluvial facies were established (Figure 5 and Table 1). The flooding degree of the delta sand body is generally weak, the oil saturation is 24.1~40.2%, and the water saturation is 28.7~46.3%, indicating no water flooding or weak flooding (Figure 5a). The water-flooding degree of the braided fluvial sand body significantly varies, from no water flooding to strong water flooding, and the variation range of the oil and water saturation measurement results is also large (Figure 5b). The submergence degree of the meandering fluvial sand body is weaker than that of the braided fluvial sand body. Following the observation of 43 sample points, only 3 samples were noted to be linked to dripping, indicating strong submergence, and most samples indicate no submergence or weak submergence (Figure 5c).

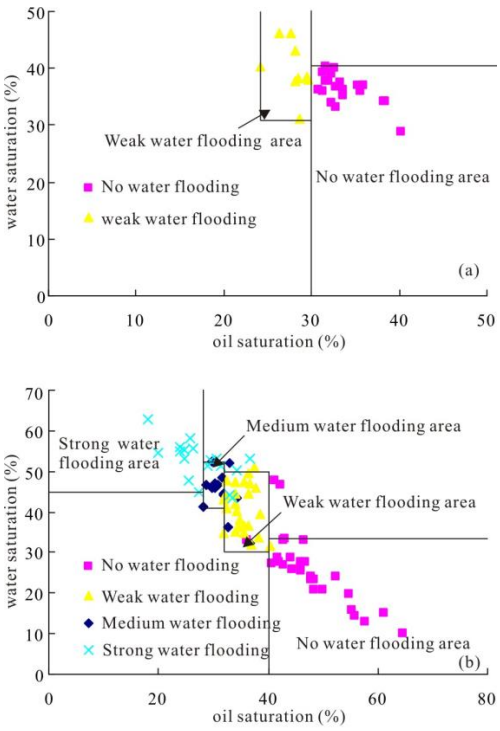


Figure 5. *Cont.*

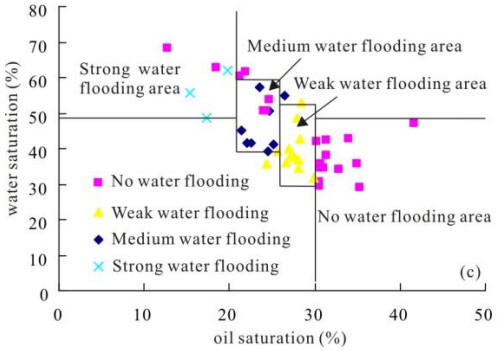


Figure 5. Identification cross-plot of water-flooding degrees by different facies of $E_2s_1^{4-7}$ in the Zhenwu area, Gaoyou Sag: (**a**) delta facies; (**b**) braided fluvial facies; (**c**) meandering fluvial facies.

Table 1. Discernment criterion of water-flooding degrees of $E_2s_1^{4-7}$ in the Zhenwu area, Gaoyou Sag.

Water-Flooding Degree	Facies					
	Delta Facies		Braided Fluvial Facies		Meandering Fluvial Facies	
	Oil Saturation	Water Saturation	Oil Saturation	Water Saturation	Oil Saturation	Water Saturation
No water flooding	>30%	<40%	>40%	<32%	>30%	<48%
Weak water flooding	24–30%	>30%	32–40%	30–50%	26–30%	30–52%
Medium water flooding	-	-	28–32%	40–52%	22–26%	39–60%
Strong water flooding	-	-	<28%	>45%	<22%	>49%

5.2. The Influence of Sedimentary Facies on Flooding Degree

There are many factors affecting the degree of flooding, with sedimentary facies representing one of the main factors [31,32].

5.2.1. Sedimentary Rhythm

Sedimentary rhythm is mainly manifested in changes in vertical particle size, and changes in particle size lead to changes in the vertical permeability of a reservoir. At the same time, different flooding modes are formed, including the bottom flooding mode of the positive rhythm, the top flooding mode of the negative rhythm, the uniform flooding mode of the homogeneous rhythm, the headquarters flooding mode of the composite positive and negative rhythm, and the top and bottom flooding modes of the composite negative rhythm.

The main oil-bearing sedimentary sand bodies in the study section are heart beaches, edge beaches, and channels, and the sedimentary rhythm is essentially a positive rhythm or compound positive rhythm. Taking the positive-rhythm sand body of the braided fluvial beach in the Zhenjian 4 well as an example, the permeability was observed to show an obvious positive rhythm. The top permeability of a rhythm set is low, and the bottom permeability is high (Figure 6). This set of rhythms consists of mudstone, silty mudstone, fine sandstone, medium-coarse sandstone, sandy conglomerate, and conglomerate. The silty mudstone and calcareous siltstone with low permeability can be further divided into three rhythm sections. The changes in the flooding degree in the three rhythms are as follows: no water flooding → weak water flooding → medium water flooding → medium–strong water flooding → strong water flooding; each positive rhythm from the top degree to the bottom flooding degree gradually weakens. This is because the porosity and permeability of the coarse sandstone and glutenite at the bottom of the positive rhythm are good, while the porosity and permeability at the top of the positive rhythm are worse than those at the bottom due to the thinning of lithology, and the injected water easily flows along

the high-permeability layer, forming the dominant channel of water flow. However, the injected water at the top advances slowly or even does not enter the water at all, resulting in weak flooding [33–35]. Because of the above reasons, in the late stage of water injection development, there is essentially no residual oil in the high-permeability layer at the bottom of the positive rhythm, but the residual oil is relatively enriched in the top and low-permeability layers. For such thick sets of positive-rhythm sand bodies, perforation mining at the top of the positive rhythm should be focused on.

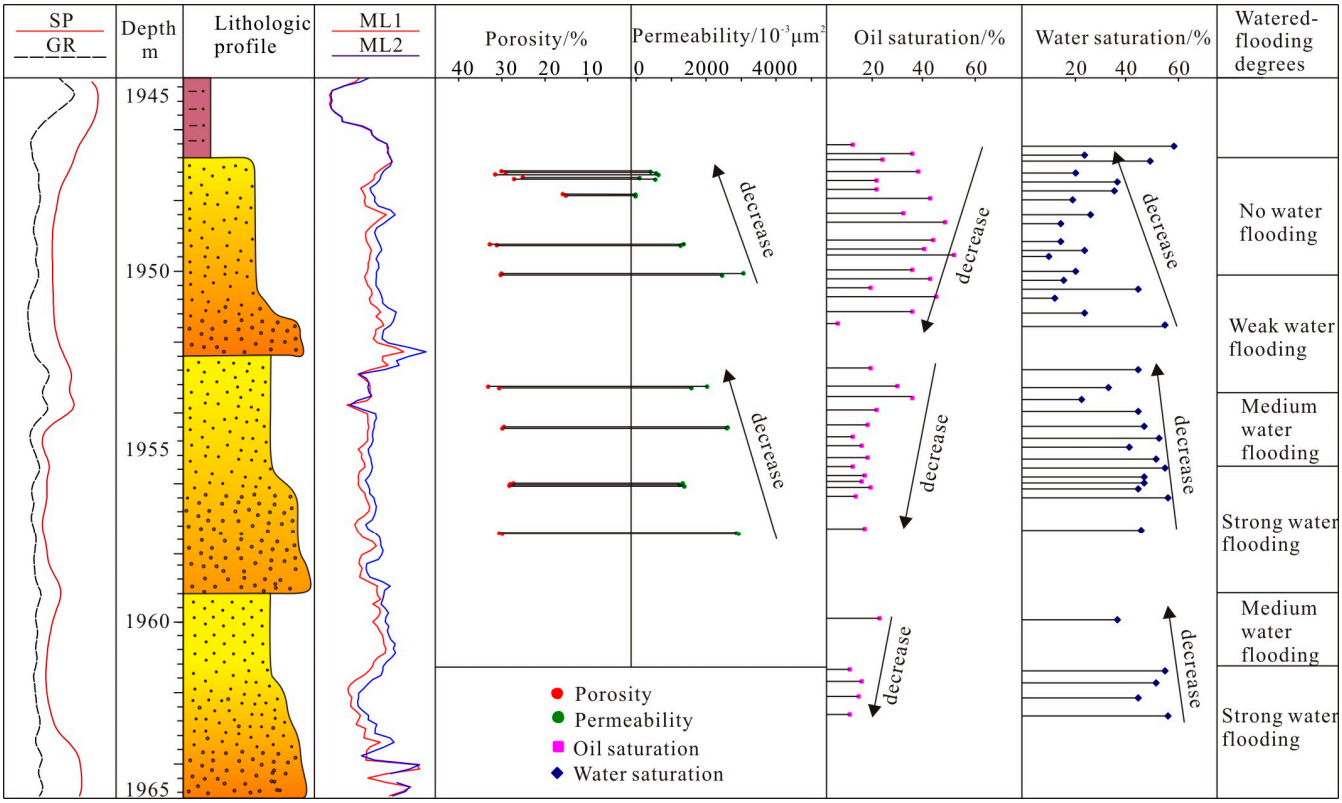


Figure 6. Influence of sedimentary rhythm on water-flooding degrees in the Zhenwu area, Gaoyou Sag.

5.2.2. Sedimentation Types

Due to the changes in the sedimentary environment, the permeabilities of the sand bodies deposited during different periods of time in the study area are quite different, resulting in different flooding degrees of different sedimentary types, and the change in the flooding degree has a high matching degree with the sedimentary types. The main sedimentary type of the oil-bearing sand body in the $E_2s_1^7$ sand group is the underwater distributary channel of the delta front. The sediments are mainly sand and silt with a fine grain size, and the reservoir has a medium physical property [36]. The oil saturation ranges between 24.1% and 40.2%, and the water saturation ranges between 27.7% and 46.3%. Oil sand dripping is essentially impermeable or slightly permeable, the flooding degree is weak, and oil enrichment remains (Figure 7a). The sedimentation of the braided fluvial facies in the six sand groups reveals the first member of the Sanduo Formation [37]. It could be observed that a large core sand body area develops, the physical properties of the reservoir's core sand body are the best, and the degree of flooding is the most serious. However, due to the rhythmic characteristics of this same core sand body, the degree of flooding also has rhythmic characteristics.

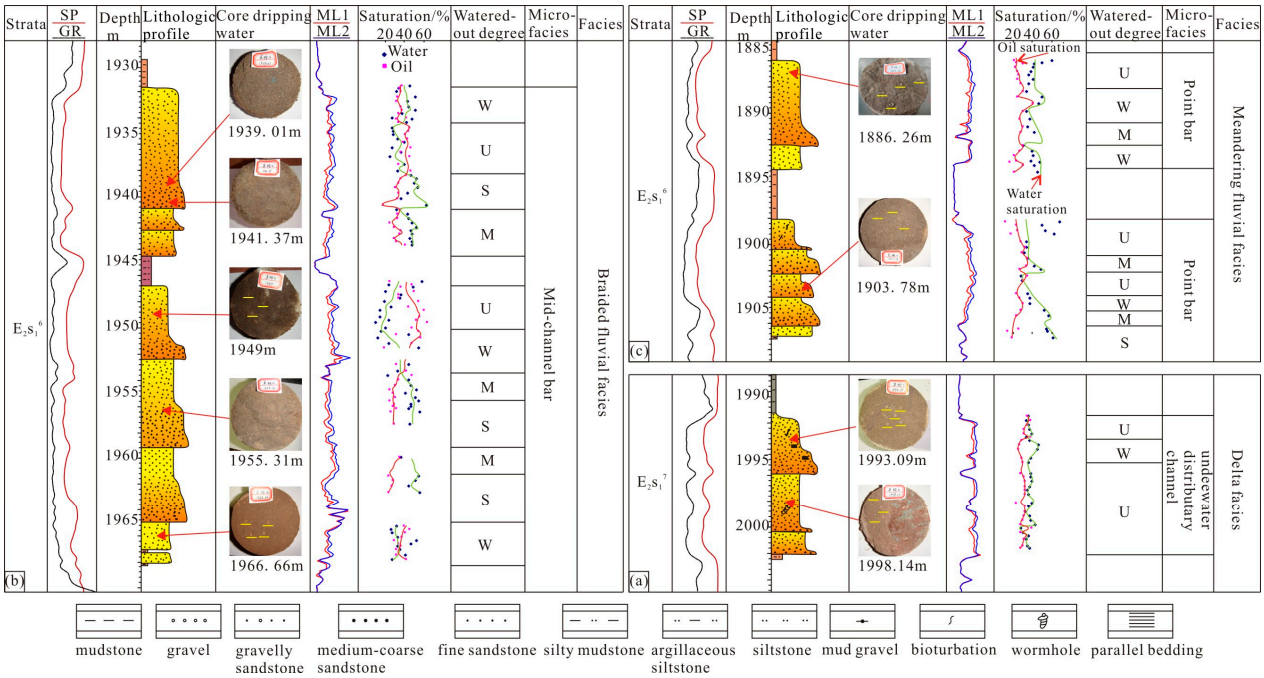


Figure 7. Influence of sedimentary type on water-flooding degrees in the Zhenwu area, Gaoyou Sag. (**a**) Delta facies; (**b**) braided fluvial facies; (**c**) meandering fluvial facies. U: no water flooding; W: weak water flooding; M: medium water flooding; S: strong water flooding.

It is easy to flood the top of the positive-rhythm core sand body, and it is difficult to flood the bottom. The remaining oil is concentrated at the top of the positive rhythm. For the same thick layer of the core sand body, due to the existence of the non-permeability deposition layer, the whole thick layer of the connected core sand body can be divided into several independent parts, which changes the traditional core sand body flooding mode. Then, the residual oil tapping in the late core beach sand body focuses on the lower part of the deposition layer and the top of the positive rhythm (Figure 7b). The $E_2s_1^{4-5}$ sand group is of a meandering fluvial deposition, and the main oil-bearing sand bodies are side shoals and rivers. The flooding form of the side shoals is similar to that of the core shoals, and it is difficult to flood the top and easy to flood the bottom. However, the development range of the side shoals is small, and they are lenticular in their profile. It is generally difficult to affect the water injection, and the flooding degree is generally weak. The river channel distribution is mainly affected by river action. The sand body is distributed in a band with good connectivity. The water saturation measured by the core is as high as 53~62.1%, and the oil saturation is only 15.4~28.5%, which denotes a strong water-flooded layer (Figure 7c).

6. Conclusions

(1) The $E_2s_1^{4-7}$ sand group in the Zhenwu area of the Gaoyou Sag has many sedimentary types and fast phase transformation. It has a set of multi-type deposits formed under the background of lake regression, mainly developing delta facies, braided fluvial facies, and meandering fluvial facies. The sand body characteristics of the various sedimentary types are different. About 35 years of water injection development has led to varying degrees of water flooding in the study area.

(2) A core scale drip experiment is carried out on the sealed core of the Zhenjian 4 well. Identification standards for the water-flooding degrees of delta facies, braided river facies, and meandering river facies are established. The water-flooding degree of the delta sand body is generally weak, and the oil saturation is 24.1–40.2%, which essentially indicates no water flooding or weak water flooding. The water-flooding degree of the braided fluvial sand body changes significantly, and the variation range

of the oil and water saturation measurement results is also large. The water-flooding degree of the meandering fluvial sand body is weaker than that of the braided fluvial sand body, which is mostly not flooded or weakly flooded.

(3) The top permeability measurement of the positive-rhythm sand bodies in the study area is low, and the bottom permeability measurement is high. The permeabilities of the sand bodies with various sedimentary types are quite different, resulting in different water-flooding degrees. Due to the existence of the non-permeable deposition layer, the whole thick layer connected to the sand body of the heart beach is divided into several independent parts, which changes the traditional water-flooding modes of the heart beach sand body. The water-flooding degree of the river is stronger than that of the sedimentary microfacies, such as the edge beach and the heart beach.

Author Contributions: Conceptualization, methodology, and validation, X.J. and X.Z.; formal analysis, X.J.; investigation, B.Z.; resources, B.Z. and R.Z.; data curation, B.Z. and X.W.; writing—original draft preparation, X.Z.; writing—review and editing, X.J. and X.Z.; visualization, D.G.; supervision, X.W.; project administration, X.J.; funding acquisition, X.Z. All authors have read and agreed to the published version of the manuscript.

Funding: This research was funded by the Young Natural Science Foundation of Xinjiang Province, China, grant number 2021D01F39.

Data Availability Statement: Not applicable.

Conflicts of Interest: The authors declare no conflict of interest.

References

1. Li, J.; Li, X.; Gao, W.; Jiang, T. Residual oil distribution research of high water-cut stage in Tuha Oilfield. *Nat. Gas Geosci.* **2005**, *16*, 378–381.
2. Jiang, Z.; Liu, Z.; Zhao, P.; Chen, Z.; Mao, Z. Evaluation of tight waterflooding reservoirs with complex wettability by NMR data: A case study from Chang 6 and 8 members, Ordos Basin, NW China. *J. Pet. Sci. Eng.* **2022**, *213*, 110436. [CrossRef]
3. Feng, C.; Bao, Z.; Chen, B.; Wei, Z.; Wang, Y. Application of the single factor analysis and multifactor coupling method to the remaining oil prediction in Fuyu Oilfield. *Acta Pet. Sin.* **2012**, *33*, 465–471.
4. Song, Z.; Tan, C.; Wu, S.; Yang, G.; Jin, X. Application of grey system theory and neural network technology to watered-out formation logging evaluation. *Pet. Explor. Dev.* **1999**, *26*, 90–92.
5. Cui, C.; Wei, S.; Wang, Z.; Qian, Y.; Wu, Z. Response time of waterflooding in low-permeability reservoirs. *Unconv. Resour.* **2022**, *2*, 85–90. [CrossRef]
6. Zhao, J.; Cheng, P.; Liu, D.; Xu, W. The application of the support vector machine to the recognition of flooding formation. *Geophys. Geochem. Explor.* **2008**, *32*, 652–655.
7. Ci, X. Study and application of logging evaluation for water-flooded zone based on fuzzy mathematics and fractal theory. *Prog. Geophys.* **2012**, *27*, 1525–1532.
8. Zhang, M.; Qi, M.; Lin, L. Integrated evaluation method of water flooded layer in ultra-low permeability reservoir in peripheral Daqing Oilfield. *Lithol. Reserv.* **2016**, *28*, 93–100.
9. He, Z.; Cui, Z.; Chen, G.; He, Y.; Wang, X. Evaluating Residual Oil Saturation and Water-flood Degree with Hydrocarbon Ratio Logging. *J. Southwest Pet. Univ.* **2016**, *38*, 41–49.
10. Shen, H.; Ma, X.; Li, H.; Wang, B.; Zhang, P.; Meng, L. A low permeable reservoir watered-out degree at the high water-cut stage identification method is discussed in this paper: To Wuliwan A reservoir as an example. *Petrochem. Ind. Appl.* **2017**, *36*, 128–130.
11. Ren, J.; Tang, J.; Chen, B.; Zhao, W. Determination of the remained oil saturation for the heterogeneous watered-out layer by the production profile date. *Pet. Geol. Oilfield Dev. Daqing* **2017**, *36*, 137–140.
12. Shi, Y.; Zhou, J.; Zhong, J.; Wang, C.; Zhong, X.; Zhang, S. Method and application fou identifying waterflooded layer with reconstructed resistivity curves. *Well Logging Technol.* **2018**, *42*, 42–48.
13. Miao, Q.; Ling, H.; Lin, Y.; Liu, J.; Xing, D. Log interpretation method for water flooded layer in a foreign oilfield. *Well Logging Technol.* **2020**, *44*, 486–490.
14. Lang, D.; Lun, Z.; Lv, C.; Wang, H. Core experimental evaluation of clastic reservoir saturation and water displacement effect: Triassic development zone in the 9th block of Tahe oilfield as an example. *CT Theory Appl.* **2021**, *30*, 311–321.
15. Zhao, B.; Hou, J.; Zhang, G.; Chen, S.; Liu, Y. Sedimentary microfacies and remaining oil distribution of the Eocene Guaduas formation in Velasquez Oilfield, Columbia. *J. Cent. South Univ.* **2011**, *42*, 1385–1392.
16. Sun, Y.; Chen, C. Control on the remaining oil distribution by reservoir sedimentary microfacies — an example from Shuanghe Oilfield. *XJPG* **2002**, *23*, 205–207.

17. Yu, H.; Wang, Y.; Zhang, L.; Zhang, Q.; Guo, Z.; Wang, B.; Sun, T. Remaining oil distribution characteristics in an oil reservoir with ultra-high water-cut. *Energy Geosci.* **2022**, 100116. [CrossRef]
18. Xing, Y.; Wang, Y.; Bai, Y.; Lin, Y.; Wang, F.; Wei, X. Sedimentary characteristics of water flooded layers and remaining oil distribution in Fuyu Oilfield. *J. Jilin Univ.* **2008**, *38*, 128–132.
19. Zhang, J.; Liu, G.; Cao, Z.; Maarten Felix, T.; Kong, Y.; Zhang, Y. Characteristics and formation mechanism of multi-source mixed sedimentary rocks in a saline lake, a case study of the Permian Lucaogou Formation in the Jimusaer Sag, northwest China. *Mar. Pet. Geol.* **2019**, *102*, 704–724. [CrossRef]
20. Noronha-D'Mello, C.A.; Nair, A.; Mahesh, B.S.; Warrier, A.K.; Mohan, R.; Kurian, S. Glacial-Holocene climate-driven shifts in lacustrine and terrestrial environments: Rock magnetic and geochemical evidence from East Antarctic Mochou Lake. *Palaeogeogr. Palaeoclimatol. Palaeoecol.* **2021**, *576*, 110505. [CrossRef]
21. Wu, S.; Tan, C. Braided delta deposition of E2S16 reservoir zones in block Zhen-12,Zhenwu Oilfield. *J. Xi'an Shiyou Univ.* **2004**, *19*, 1–4.
22. Hou, L.; Wang, J.; Liu, Z. Evaluation of water flooded interval well logging. *Acta Pet. Sin.* **1999**, *20*, 49–55.
23. Lei, X.; Zhao, C.; Zhang, Q.; Wang, P.; Xiong, R. Effect of high-multiple water injection on rock pore structure and oil displacement efficiency. *Energy Geosci.* **2022**, 100137. [CrossRef]
24. Tan, F.; Li, H.; Wu, X.; Fan, X.; Yu, H. Quantitative identification of water-flooded zones in conglomerate reservoirs—An example from theKexia Formation in the Liuzhong block of Karamay Oilfield. *Oil Gas Geol.* **2010**, *31*, 232–239.
25. Tan, B.; Luca, C.; Nigel, P. Quantitative characterization of the sedimentary architecture of Gilbert-type deltas. *Sediment. Geol.* **2021**, *426*, 106022. [CrossRef]
26. Zhen, D.; Zai, X.; Jiang, G. Sedimentary characteristics, genetic types and control factors of deep-water sandstones in the western Lijin Sag, China. *Mar. Pet. Geol.* **2020**, *113*, 104130.
27. Zhen, H.; Wei, W.; Shang, W.; Chen, H.; Reza, R.; Jia, C. Impacts of gas properties and transport mechanisms on the permeability of shale at pore and core scale. *Energy* **2022**, *244*, 122707.
28. Feng, C.; Shan, Q.; Shi, W.; Zhu, W. Reservoirs heterogeneity and its control on remaining oil distribution of K_1q_4, Fuyu Oilfield. *J. China Univ. Pet.* **2013**, *37*, 1–7.
29. Lu, G.; Zhang, L.; Liu, Q.; Xu, Q.; Zhao, Y.; Li, X.; Deng, G.; Wang, Y. Experiment analysis of remaining oil distribution and potential tapping for fractured-vuggy reservoir. *J. Pet. Sci. Eng.* **2022**, *208*, 109544. [CrossRef]
30. Zhao, X.; Zhang, S.; Yang, S.; Ju, X.; Chen, G.; Zhang, X.; Khan, D.; Zhang, Y.; Zhang, J. Controlling factors of carbonate cement and its influence on oil-water distribution of the Neoene Shawan Formation in the northern Chepaizi area, Junggar Basin, NW China. *J. Pet. Sci. Eng.* **2021**, *206*, 108942. [CrossRef]
31. Zhang, S.; Liu, Z.; Jin, B.; Liu, H.; Dong, C.; Zhang, W. Formation of paleogene lithologic reservoir and distribution in Gaoyou sag, Subei basin. *Nat. Gas Geosci.* **2012**, *23*, 99–105.
32. Zhou, J.; Lin, M.; Zhang, X.; Yao, Y.; Pan, F.; Yu, H.; Chen, S.; Zhang, M. Provenance system and sedimentary facies of the Member 1 of Paleogene Dainan Formation in Gaoyou Sag, Jiangsu Province. *J. Palaeogeogr.* **2011**, *13*, 161–174.
33. Josep, P.; Mayte, B. Fault-slip, bed-length and area variations in experimental rollover anticlines over listric normal faults: Influence in extension and depth to detachment estimations. *Tectonophysics* **2005**, *396*, 97–117.
34. Jian, T.; Yi, L.; Li, J.; Na, J.; Zhi, Y.; Ping, L. Investigation on water phase trapping mechanisms in tight gas reservoirs: Pore-scale visualization observation and core-scale flooding analysis. *J. Pet. Sci. Eng.* **2021**, *198*, 108185.
35. Huang, C.; Janok, P. Facies analysis and its relation to point-sourced growth faults in river-dominated prodeltaic delta front deposits of the Cretaceous Ferron Notom Delta, Utah, USA. *Mar. Pet. Geol.* **2017**, *81*, 237–251. [CrossRef]
36. Zhao, X.; Wang, S.; Yang, J.; Zhang, B.; Li, L.; Liu, X.; Wen, W.; Zhang, Y. Evaluation method for low- to ultralow-permeability reservoirs based on pore-throat structure: A case study in the eastern Nanpu Sag, Bohai Bay Basin, China. *Interpretation* **2021**, *9*, T315–T329. [CrossRef]
37. Wei, X.; Zhang, T.; Liang, X.; Yao, Q.; Tang, X. Sedimentary characteristics and evolution of the 1stmember of Dainan Formation and the 1stmember of Sanduo Formation in Qutang and Haibei Sub-sags Hai'an Sag. *Oil Gas Geol.* **2012**, *33*, 265–276.

Disclaimer/Publisher's Note: The statements, opinions and data contained in all publications are solely those of the individual author(s) and contributor(s) and not of MDPI and/or the editor(s). MDPI and/or the editor(s) disclaim responsibility for any injury to people or property resulting from any ideas, methods, instructions or products referred to in the content.